Loss Breakdown of a Dual Conical Rotor Permanent Magnet Motor using Grain Oriented Electrical Steel and Soft Magnetic Composites

Matthew C. Gardner
Dept. Elec. & Comp. Engr.
Texas A&M University
College Station, TX, USA
gardner1100@tamu.edu

Yichi Zhang
Dept. Elec. & Comp. Engr.
Texas A&M University
College Station, TX, USA
peterzhanghs@gmail.com

Dorsa Talebi
Dept. Elec. & Comp. Engr.
Texas A&M University
College Station, TX, USA
dorsa.talebi@tamu.edu

Hamid A. Toliyat
Dept. Elec. & Comp. Engr.
Texas A&M University
College Station, TX, USA
toliyat@tamu.edu

Alan Crapo
Regal Beloit® Corporation
Beloit, WI, USA
Alan.Crapo@regalbeloit.com

Paul Knauer
Regal Beloit® Corporation
Beloit, WI, USA
Paul.Knauer@regalbeloit.com

Harold Willis
Regal Beloit® Corporation
Beloit, WI, USA
harold.willis@regalbeloit.com

***Abstract*—This paper provides a loss breakdown of the NovaMAX® 215 frame, 1800 rpm motor at 5 kW. Mechanical losses, copper loss, and various types of electromagnetic losses are identified through experiment and simulation. The motor is able to achieve a very high efficiency, up to 96% at some operating points. A comparison with another highly efficient permanent magnet motor illustrates the benefits of the dual rotor axial flux topology, the use of grain oriented electrical steel, and the conical air gap and rotor flux focusing topology together with ferrite magnets. Additionally, a motor with a variable air gap was tested at different air gaps, and its losses are shown. At low speed and high torque, the losses are minimized with relatively small air gaps. However, at higher speeds and lower torques, the optimal air gaps are larger.**

Keywords*— *Axial flux, conical rotor, dual rotor, efficiency, flux concentration, grain oriented electrical steel, losses, motor, permanent magnet, soft magnetic composite

I. Introduction

The US Department of Energy (DOE) Advanced Manufacturing Office's Next Generation Electric Machines: Enabling Technologies program seeks to develop ways to employ high performing materials to improve the efficiency of motors without depending on large quantities of rare earth materials [1]. Regal Beloit's NovaMAX motor incorporates several innovations to achieve very high efficiencies. As shown in Fig. 1, the NovaMAX motor is a dual-rotor permanent magnet (PM) motor with conically shaped air gaps.

Grain oriented electrical steel (GOES) provides higher permeability, higher saturation flux density, and lower core losses than nonoriented electrical steel when the flux is primarily in the direction of the grain orientation. Thus, GOES is frequently used in transformer cores; however, because most motors employ a rotating magnetic field, nonoriented steel is used in the vast majority of motors. Nonetheless, GOES has been applied to motors in a few studies [2]-[6], but the manufacturing complexity of the motor is often increased to accommodate the GOES [2]-[5]. However, as in [6], the dual rotor axial topology results in the individual stator teeth only being exposed to a pulsating axially directed flux, rather than a rotating flux, so the teeth in the NovaMAX motor are well suited for using GOES.

Additionally, the NovaMax motor employs a flux concentrating rotor topology. As illustrated in Fig. 1(b), flux

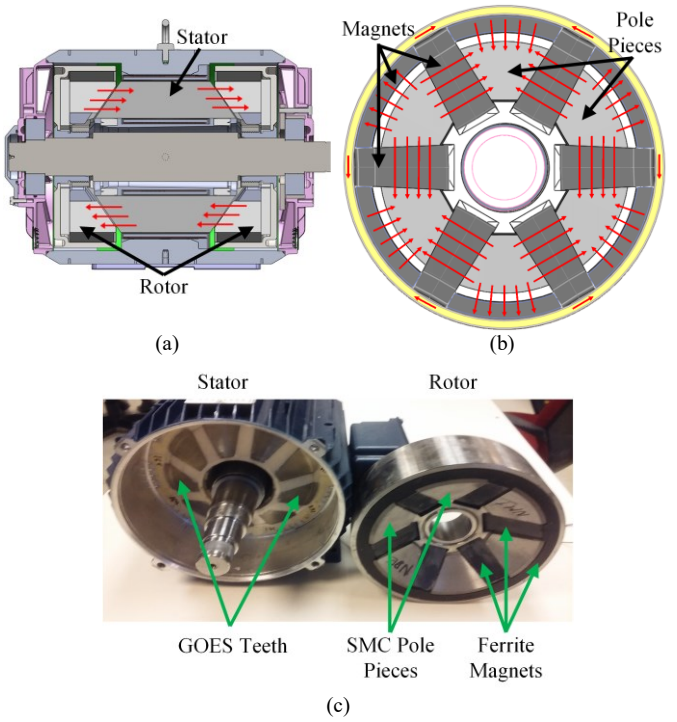

Fig. 1. NovaMAX motor (a) transverse-section view with red arrows illustrating flux direction, (b) cross-section view of one rotor with red arrows illustrating flux direction, and (c) view with one rotor removed.

This work was supported by the US Department of Energy under award number DE-EE0007875.

from PMs in multiple directions is concentrated in soft magnetic composite (SMC) pole pieces in each rotor before crossing the air gap to the stator. Furthermore, the conical shape of the air gap results in a larger surface area relative to an axial flux motor with the same diameter. This increased air gap surface area reduces the reluctance of the flux path, resulting in an increase in flux traveling from the rotor to the stator. These effects result in high stator flux densities, even though ferrite magnets are used instead of rare earth magnets. Since ferrite magnets have high resistivity, this also eliminates the eddy current losses that would be present in rare earth magnets. The adoption of SMCs in motors has been limited because SMCs have lower permeability, lower saturation flux density, and higher hysteresis losses than steel laminations [7]-[8]. However, SMCs have a significant advantage over laminations because its properties are relatively isotropic, whereas steel laminations have lower permeability and high eddy current losses for flux normal to the laminations. Thus, SMCs have been used in motors for places where the flux paths are inherently three dimensional [8]-[10]. The flux concentration topology and the conical air gap result in flux travelling in all directions in the NovaMAX® rotors, so the rotor pole pieces should be made of SMC, rather than laminations. Additionally, since the flux changes on the rotor are relatively small, the hysteresis losses in the SMC are relatively minor.

This paper presents a detailed loss breakdown of the current NovaMAX 215 frame size, 1800 rpm motor as the first step in the process of the DOE program to raise the efficiency of a 5 kW, 1800 rpm motor. The experimental test setup is shown in Fig. 2. The motor under test (MUT) is driven by a Yaskawa A1000 variable frequency drive (VFD) operating at a switching frequency of 4 kHz. During initial testing, the switching frequency of the drive was varied between 4 kHz and 10 kHz, but this had a very minimal impact on the losses. The mechanical load is provided by a Marathon Black Max induction generator controlled by a Yaskawa U1000 VFD. The mechanical power is measured by a Himmelstein MCRT 49802V torque meter, and the electrical power input to the MUT is measured using a Yokogawa PZ4000 power analyzer. Simulation results from a commercial 3D finite element analysis (FEA) software, ANSYS Maxwell, are used to provide better detail on the separation of losses than can be determined solely using experimental results. Because there are some uncertainties regarding material properties, especially after machining operations, and the temperatures of each part of the motor during operation, coefficients are used to slightly adjust the various simulated loss components to fit the experimental data more closely, using a least-squares curve fit.

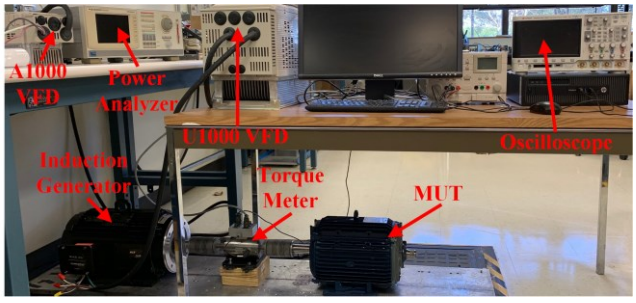

Fig. 2. Experimental test setup with protective enclosure removed.

II. Mechanical Losses

Friction and windage both contribute to the mechanical losses. To isolate these losses, the torque meter and mechanical load were disconnected, and no-load spindowns were performed with both a normal motor and a motor with a nonmagnetized rotor. Since the inertia of the rotor is known, the loss can be calculated by measuring the rate of deceleration of the motor, which was determined from the back-emf waveforms measured using the Keysight DSO-X 3024A oscilloscope shown in Fig. 2. In the case of the non-magnetized motor, both motor shafts were mechanically connected together, and the rate of deceleration was determined from the back-emf of the normal motor. Then, the normal motor's losses were subtracted from the total losses to determine the losses of the nonmagnetized motor. Fig. 3 illustrates the room temperature no-load losses of the normal motor and the nonmagnetized motor. The normal motor was tested with and without both a fan and a seal. The non-magnetized motor was tested without fans or seals. Additionally, since the non-magnetized motor was not being supplied by an inverter, its shaft grounding brush could be removed. Based on these tests, the room-temperature mechanical losses from the fan, seals, and brush at 1800 rpm could be identified as approximately 9 W for the fan, 16 W for each seal, and 3 W for the shaft grounding brush. For all results presented after this point, the fan and seals have been removed from the motor to simplify the identification of losses.

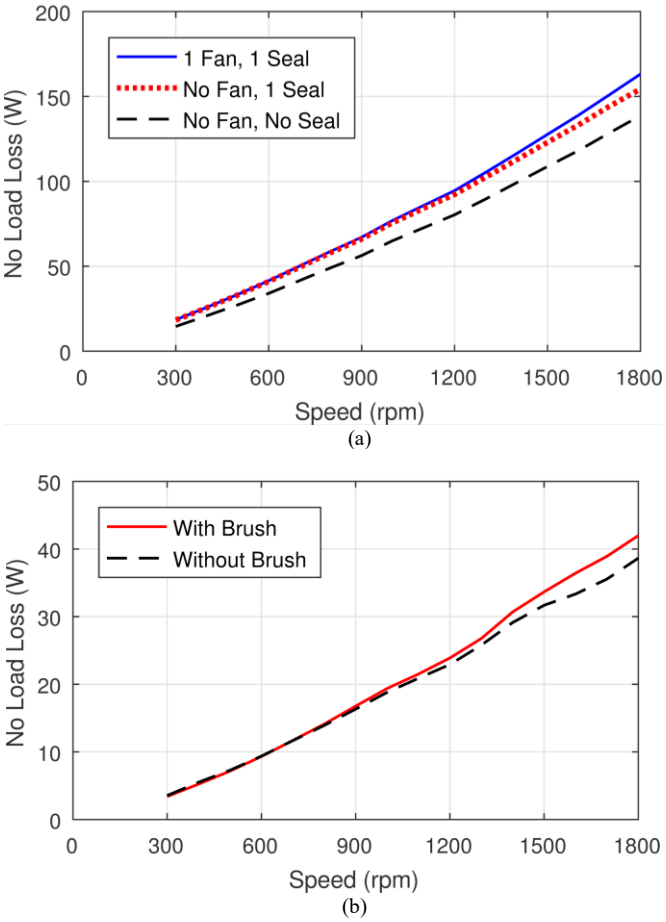

Fig. 3. Room temperature no-load losses in (a) the normal motor and (b) the nonmagnetized rotor.

While the previous losses were determined at room temperature, the bearing losses change significantly with temperature because the viscosity of the bearing grease is affected by bearing temperature. Fig. 4(a) illustrates the no-load loss in the normal motor without fans or seals across a range of temperatures measured on the end plates near the bearings. However, the core losses also decrease as the temperature increases because the magnets produce less flux as they become warmer. Fig. 4(b) illustrates the impact of the reduced flux on the back emf as the housing temperature increases. (Based on the results in Fig. 4(b), the remanence of the PMs in the FEA was decreased by 8% from the nominal remanence at room temperature.) Therefore, the bearing losses at the nominal operating temperature are calculated using the formula provided by SKF [11] for shielded 6308 bearings. Fig. 5 shows the calculated bearing losses from both bearings versus speed after the adjustment to compensate for the uncertainties in bearing temperature and exact axial loading on each bearing.

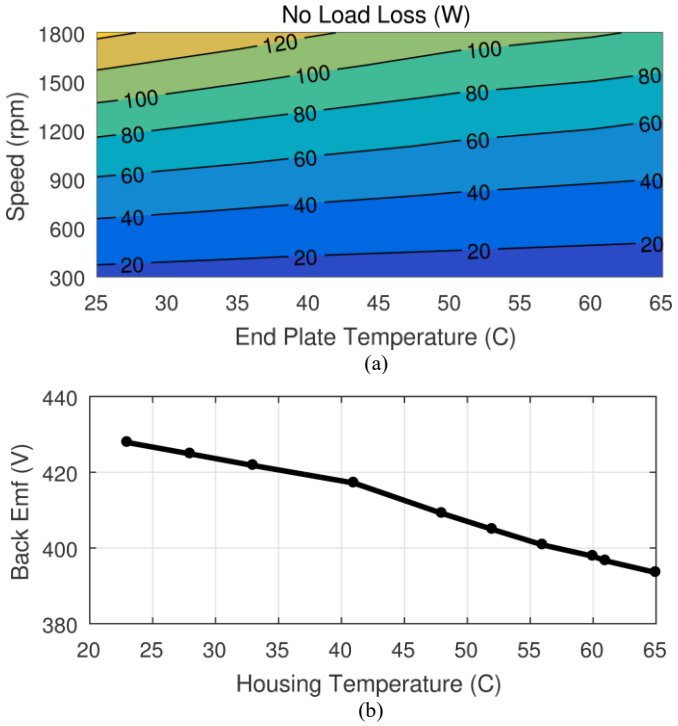

Fig. 4. Variation of (a) no load loss with end plate temperature and speed for the motor with no fan or seals and (b) line-to-line rms back emf at 1800 rpm with housing temperature.

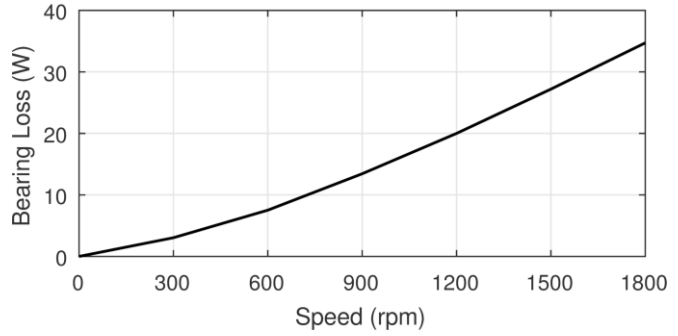

Fig. 5. Calculated bearing loss from both bearings at the nominal operating temperature.

III. Copper Losses

Copper losses also contribute significantly to the overall losses in the MUT. Fig. 6(a) shows the phase currents measured at different torques and speeds, and Fig. 6(b) shows the computed copper losses. The line-to-line resistance was measured to be 0.63 Ω at 22.5 °C. However, the MUT was run at the nominal operating point of 5 kW at 1800 rpm until the motor reached thermal equilibrium (about 60 °C on the motor housing) before taking these measurements. A thermocouple placed on the outside of the coil insulation measured temperatures very close to those measured on the surface of the case. However, the insulation results in a significant temperature difference between the copper and the thermocouple; additionally, a measurement at a single point may not accurately reflect the average temperature of the entire windings. Based on the least-squares fit, the actual line-to-line resistance at thermal equilibrium was 0.75 Ω, which would correspond to an average copper temperature of 71 °C. Fig. 6 illustrates that the current and copper loss depend primarily on the torque with little impact from the speed and that the torque is very linear with current up to 30 N·m.

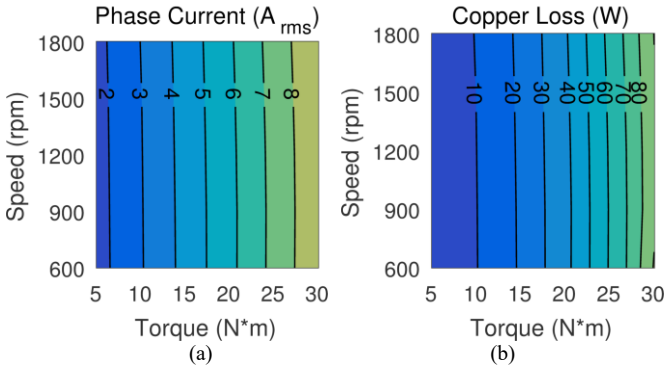

Fig. 6. (a) Measured rms phase currents and (b) calculated copper loss at thermal equilibrium.

IV. Electromagnetic Losses

The changing flux also creates significant electromagnetic losses in the MUT. The primary sources of electromagnetic losses in this motor are the core losses in the GOES stator teeth and the SMC rotor poles and eddy current losses in the aluminum housing. Since it is not practical to experimentally separate these different loss components, a commercial FEA package, ANSYS Maxwell, was used to simulate the electromagnetic loss components. Due to the uncertainty in material properties, especially after machining, the Steinmetz coefficients for these various loss components were slightly adjusted during the least-squares fit. Fig. 7 shows the simulation results for these loss components. Based on the simulation results, the primary source of electromagnetic losses is the core loss in the stator teeth. The losses in the SMC rotor poles are much smaller, so the higher hysteresis loss of SMC relative to laminated steel is not significantly harming motor performance. Additionally, there are some small eddy current losses in the aluminum housing; because these losses depend significantly on torque, they are likely caused by leakage flux from the stator winding.

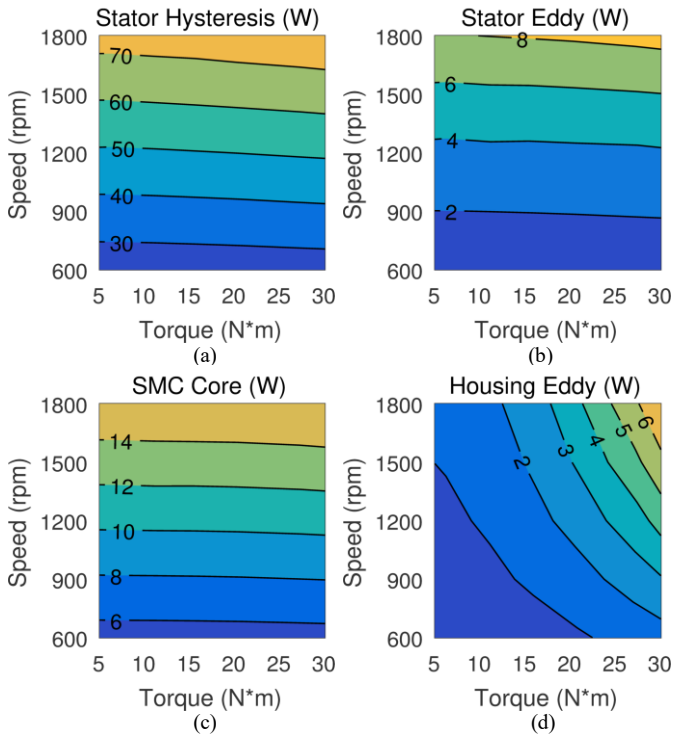

Fig. 7. Simulated (a) hysteresis and (b) eddy current losses in the GOES stator teeth, (c) core loss in the SMC rotor poles, and (d) eddy current loss in the aluminum housing.

Figs. 8 and 9 illustrates the total losses and efficiency of the MUT. Fig. 8 shows a good agreement between the simulated losses and the experimental losses, except at the highest torque measurement at 600 rpm. (At this point, the drive was not maintaining a constant torque, so the accuracy of the experimental data is poor.) Fig. 9 illustrates that the MUT is able to achieve slightly over 96% efficiency at the nominal 1800 rpm, 5 kW operating point. Additionally, it maintains a relatively high efficiency at lower speeds. However, because the core losses and bearing losses, both of which do not vary significantly with speed, produce a large portion of the losses, the efficiency does reduce somewhat at lower torques.

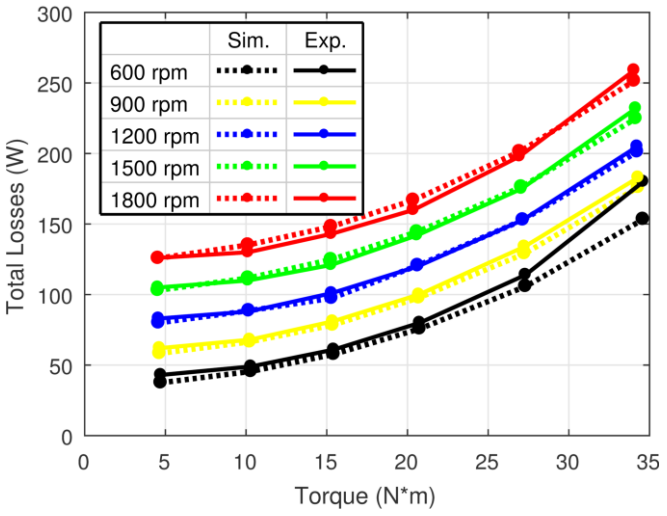

Fig. 8. Comparison of simulated and experimental losses.

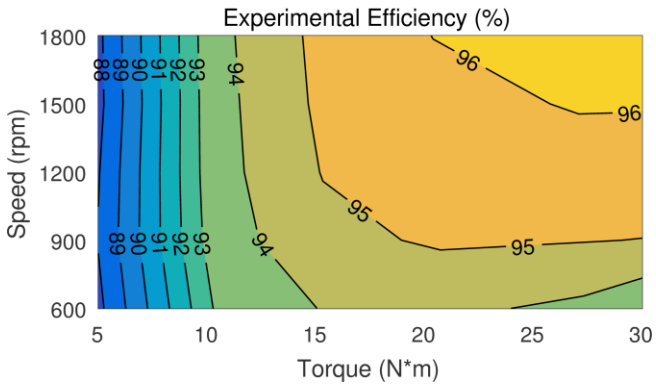

Fig. 9. Variation of experimental efficiency with torque and speed.

V. Loss Breakdown Comparison

To highlight the impact of some of the innovations in the NovaMAX® motor and their impact on losses, the NovaMAX's losses are compared with another high-efficiency motor. The ZEUS™ motor, which is rated for 11 kW at 1800 rpm, is a highly efficient radial flux motor with surface mounted rare earth PMs on the rotor [12]. Since larger motors tend to be able to achieve higher efficiencies, this does give the ZEUS motor a small advantage relative to the NovaMAX motor. Fig. 10 shows the experimentally measured efficiency of the ZEUS motor, and Table I provides a comparison between the loss breakdowns of the NovaMAX and ZEUS motors at their nominal operating point [12]. In Table I, stator core loss includes the losses in the stator teeth and the eddy current losses in the housing, and the fan and seals are not included in the friction and windage losses for the NovaMAX motor. The losses are expressed as percentages of the output power.

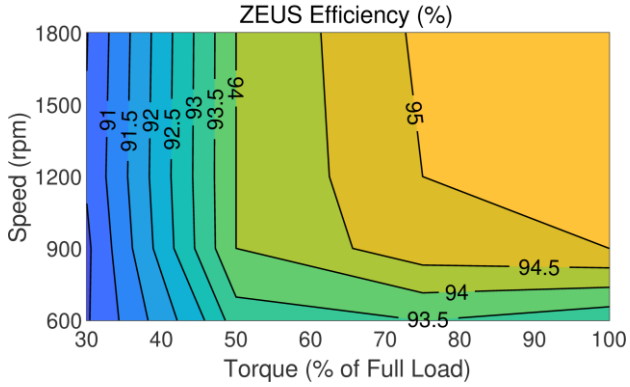

Fig. 10. Variation of ZEUS™ motor efficiency with torque and speed [12].

TABLE I. Loss Breakdown Comparison

	NovaMAX	ZEUS
Output Power	5000 W	11470 W
Speed	1800 rpm	1800 rpm
Copper Loss	1.30%	0.85%
Stator Core Loss	1.73%	2.07%
Magnet Loss	0.00%	0.35%
Rotor Core Loss	0.30%	0.32%
Friction and Windage	0.69%	0.44%
Efficiency (%)	**96.1%**	**96.1%**

Both the NovaMAX® and ZEUS™ motors achieve similar efficiencies, although the ZEUS motor's experimentally measured efficiency is a bit lower than predicted by the analysis presented in Table I [12]. However, the approaches to achieving this high efficiency are different. The ZEUS motor employs rectangular wires to achieve a high copper fill factor and reduce the copper losses, whereas the NovaMAX motor employs conventional circular wires. The NovaMAX motor achieves low core losses in the stator by eliminating the stator yoke and using GOES; however, the ZEUS motor limits the peak flux densities in the stator teeth and yoke to 1.5 T and 0.9 T, respectively, whereas the NovaMAX motor has a slightly higher peak flux density of 1.6 T in the stator teeth, but the ZEUS motor still has more stator core losses than the NovaMAX motor. The NovaMAX motor has no magnet losses because its ferrite magnets have high resistivity, whereas the ZEUS motor employs axial segmentation to mitigate the losses in its rare earth magnets.

VI. Air Gap Study

Additionally, a prototype NovaMAX motor was constructed such that the air gaps on each side could be modified. Loss data was collected for this prototype at several different air gaps to provide further data for curve fitting the loss components and to compare with the data for the nominal motor, which has air gaps of 1.15 mm and 1.6 mm. However, the construction of the air gap study motor results in the magnetic force on each rotor being applied to their respective bearings, instead of only the net magnetic force contributing to the axial forces on the bearings. Therefore, the axial forces measured in previous experiments are used in the calculation of the bearing losses, which are shown in Fig. 11 as a function of speed and air gap.

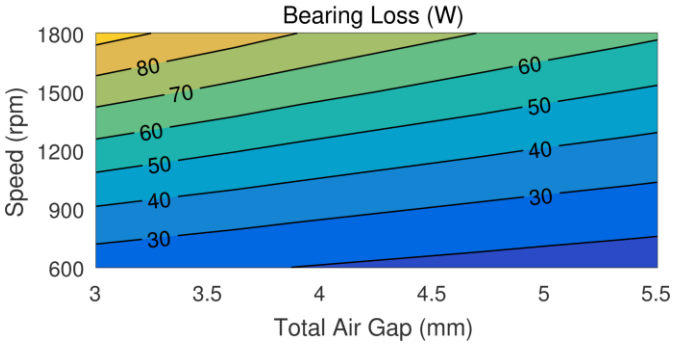

Fig. 11. Variation of calculated bearing losses in the air gap study motor.

Additionally, the actual air gaps in the gap study motor could not be physically measured. Therefore, the air gaps were determined by comparing the measured torque per amp coefficient of the motor with simulations at different air gaps. As the air gap increases, the flux in the stator from the rotor PMs reduces, which reduces the torque per amp coefficient and the back emf, as shown in Fig. 12. Thus, as the air gap increases, copper losses must increase for a given torque, whereas the other electromagnetic losses diminish due to the reduced flux linkage between the stator and the rotor. Fig. 12(b) also shows that increasing the air gap reduces the harmonic distortion present in the back emf waveform, which can further reduce core losses. Fig. 13 shows the impact of the air gap on copper losses and other electromagnetic losses.

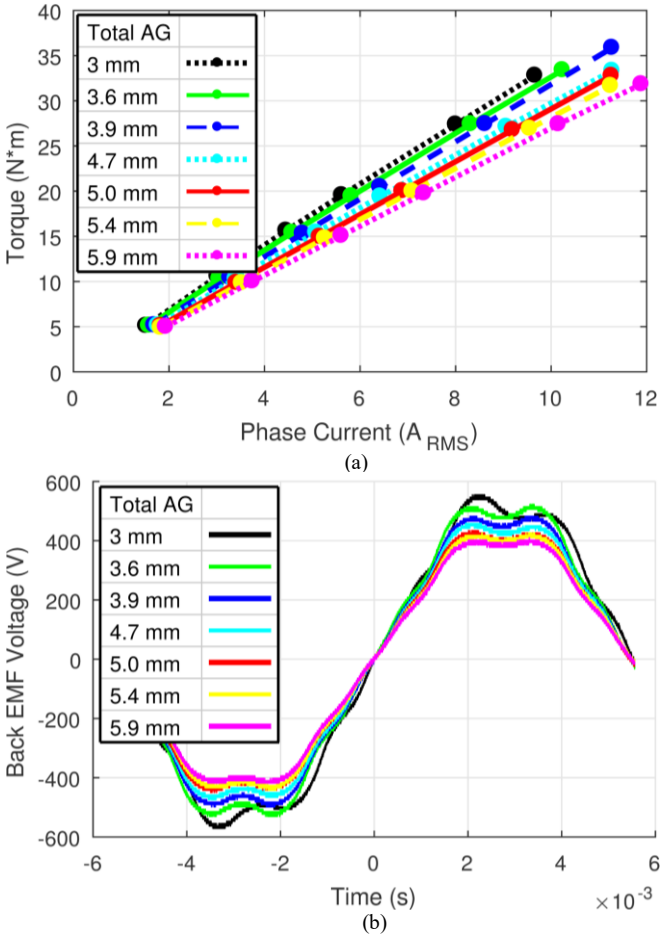

Fig. 12. Variation of (a) torques at different currents at 1800 rpm and (b) back emf at 1800 rpm with different total air gaps.

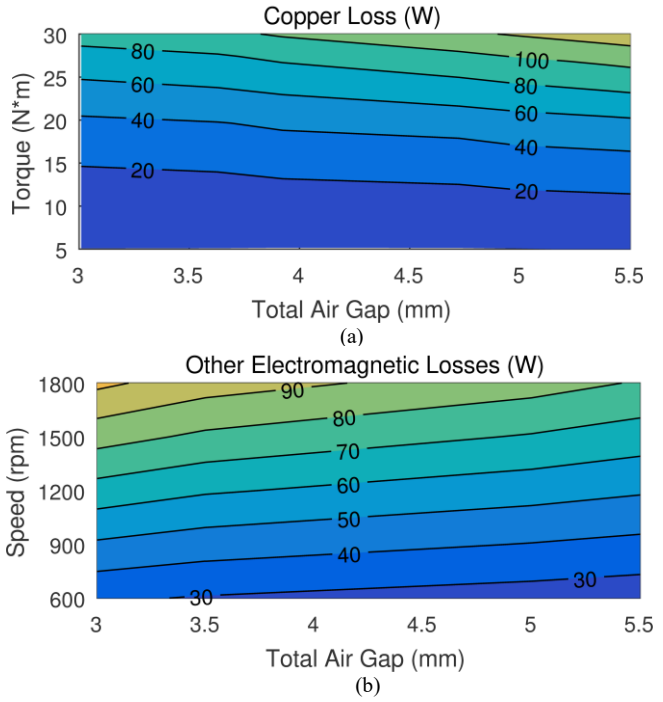

Fig. 13. Variation of (a) copper loss with torque and total air gap at 1800 rpm and (b) other electromagnetic losses with speed and total air gap near 26.5 N·m.

Fig. 14 illustrates the measured losses at different air gaps. Fig. 14 shows that, at low-speed, high-torque operation, where copper losses tend to be the dominant source of loss, the total losses are minimized with relatively small air gaps, whereas, at high-speed, low-torque operation, where other electromagnetic losses are larger than the copper losses, losses are minimized with larger air gaps. All of these cases achieve lower efficiencies than the normal NovaMAX® motor because the construction of the gap study motor results in larger bearing loss due to the larger axial forces on the bearings, especially at smaller total air gaps. Therefore, to provide a better representation of the losses if the motor was built in the conventional manner with different total air gaps, Fig. 15 shows the experimentally measured losses in the air gap study motor with the calculated bearing losses for the air gap study motor subtracted out and replaced with the calculated bearing losses for the normal motor. This bearing loss substitution reduces the anticipated losses and the optimal air gap for the best efficiency at the nominal operating point. As the same rotor and stator geometries are used for machines with different windings, which yield different torque and speed ratings, this data indicates that significant energy savings could be achieved by using different sets of shims to provide a larger air gap for higher speed machines and a smaller air gap for lower speed machines.

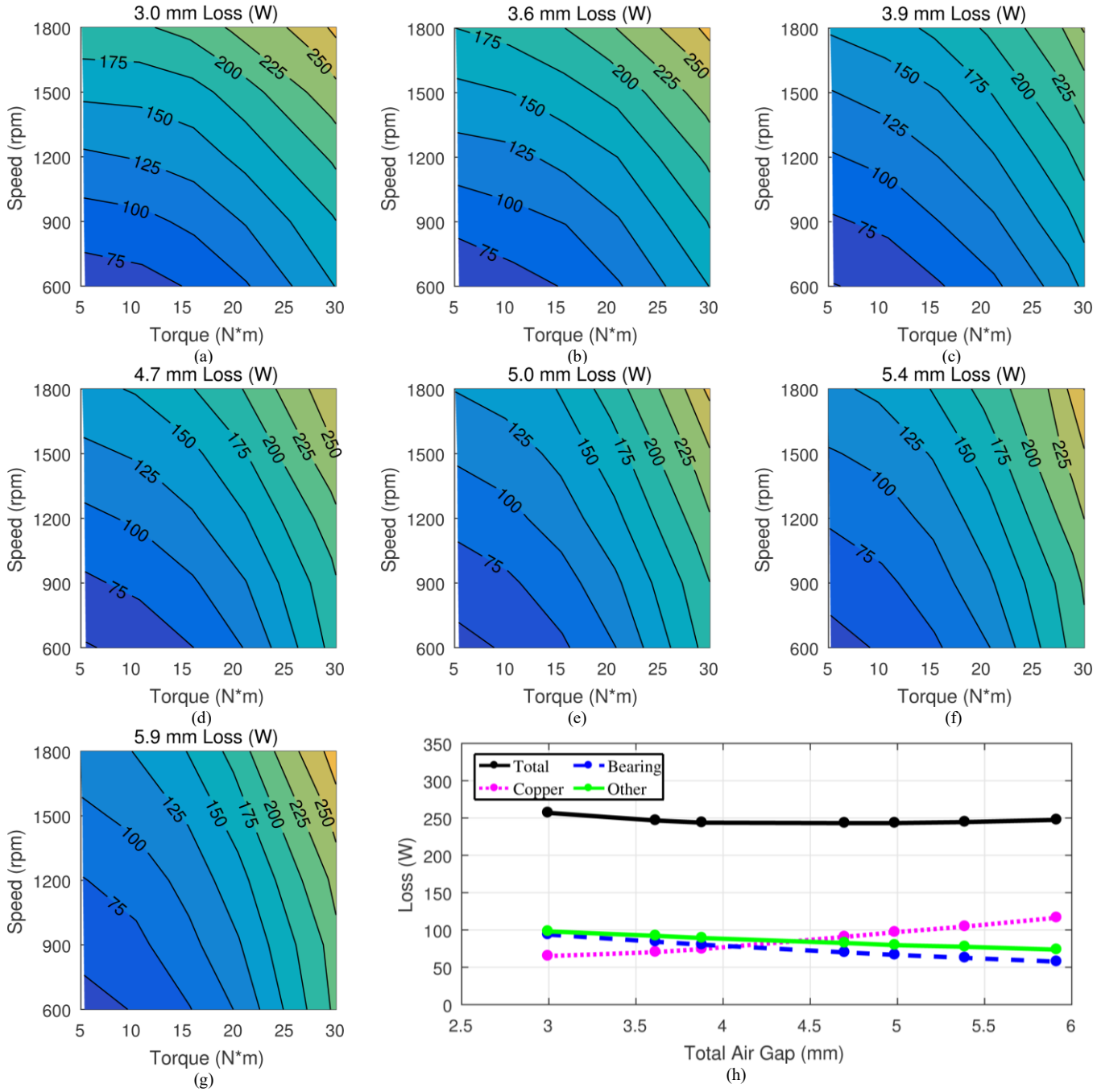

Fig. 14. Variation of (a) – (g) measured losses with torque and speed for different total air gaps and (h) calculated loss components at the nominal operating point with total air gap.

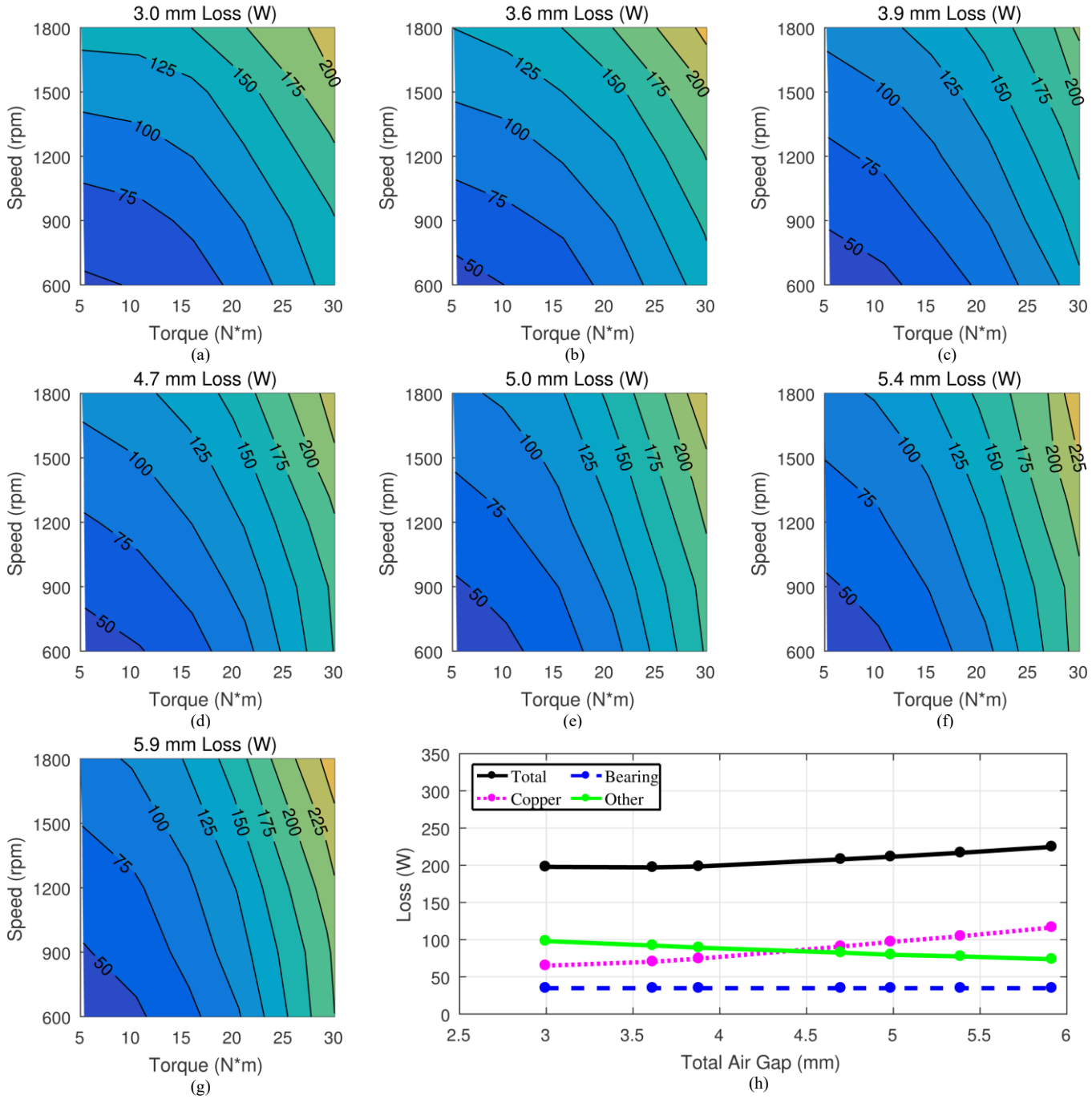

Fig. 15. Variation of (a) – (g) estimated losses with torque and speed for a normal motor with different total air gaps and (h) calculated loss components at the nominal operating point with total air gap. The estimates are produced by subtracting the calculated bearing losses from the experimental losses of the air gap study motor and replacing those bearing losses with the calculated bearing losses for the normal motor.

VII. Conclusion

The losses of a NovaMAX® motor have been measured and the loss breakdown presented. The NovaMAX motor achieves slightly more than 96% efficiency at the nominal operating point of 5 kW at 1800 rpm. Comparing the NovaMAX motor to a highly efficient radial flux surface mounted PM motor shows the impact of the innovations in the NovaMAX motor. The dual rotor axial topology allows the elimination of the stator yoke and the use of GOES for the stator teeth, which reduces core loss without sacrificing flux density in the stator. Also, the conical air gap and the rotor topology concentrate flux from the PMs so that high flux densities can be achieved with ferrite, instead of using rare earth PMs. This eliminates any eddy current loss in the PMs.

Additionally, a study was performed where the losses were measured with different air gaps. Increasing the air gap results in larger copper losses for a given torque but lower core losses

for a given speed. Thus, the optimal air gaps were relatively small for low-speed, high-torque operating points, whereas the optimal air gaps for high-speed, low-torque operating points were larger. Therefore, using different shims to create different air gaps for different speed machines with the same rotor and stator geometries could produce significant energy savings.

ACKNOWLEDGMENT

This material is based upon work supported by the Department of Energy under Award Number DE-EE0007875. This report was prepared as an account of work sponsored by an agency of the United States Government. Neither the United States Government nor any agency thereof, nor any of their employees, makes any warranty, express or implied, or assumes any legal liability or responsibility for the accuracy, completeness, or usefulness of any information, apparatus, product, or process disclosed, or represents that its use would not infringe privately owned rights. Reference herein to any specific commercial product, process, or service by trade name, trademark, manufacturer, or otherwise does not necessarily constitute or imply its endorsement, recommendation, or favoring by the United States Government or any agency thereof. The views and opinions of authors expressed herein do not necessarily state or reflect those of the United States Government or any agency thereof.

Portions of this research were conducted with the advanced computing resources provided by Texas A&M High Performance Research Computing.

The authors would like to thank ANSYS for their generous support of the EMPE lab through the provision of FEA software.

REFERENCES

[1] "DE-FOA-0001467: Next Generation Electric Machines: Enabling Advanced Technologies," Office of Energy Efficiency and Renewable Energy (EERE), Mar. 9, 2016.

[2] J. Ma, J. Li, H. Fang, Z. Li, Z. Liang, L. Xiao, and R. Qu, "Optimal Design of an Axial-Flux Switched Reluctance Motor with Grain-Oriented Electrical Steel," *IEEE Trans. Ind. Appl.*, vol. 52, no. 6, pp. 5327 – 5337, Nov./Dec. 2017.

[3] Y. Sugawara and K. Akatsu, "Characteristics of a Switched Reluctance Motor using Grain-Oriented Electric Steel Sheet," in *Proc. IEEE Int. Conf. Elect. Mach. Sys.*, 2013, pp. 18 – 23.

[4] R. Pei, L. Zeng, S. Li, and T. Coombs, "Studies on grain-oriented silicon steel used in traction motors," in *Proc. IEEE Int. Conf. Elect. Mach. Sys.*, 2017, pp. 1 – 4.

[5] S. Taghavi and P. Pillay, "A Novel Grain-Oriented Lamination Rotor Core Assembly for a Synchronous Reluctance Traction Motor with a Reduced Torque Ripple Algorithm," *IEEE Trans. Ind. Appl.*, vol. 52, no. 5, pp. 3729 – 3738, Sep./Oct. 2016.

[6] D. Kowal, P. Sergeant, L. Dupre, and A. Van den Bossche, "Comparison of Nonoriented and Grain-Oriented material in an Axial Flux Permanent-Magnet Machine," *IEEE Trans. Magn.*, vol. 46, no. 2, pp. 279 – 285, Feb. 2010.

[7] G. Cvetkovski and L. Petkovska, "Performance Improvement of PM Synchronous Motor by Using Soft Magnetic Composite Material," *IEEE Trans. Magn.*, vol. 44, no. 11, pp. 3812 – 3815, Nov. 2008.

[8] A. Krings, M. Cossale, A. Tenconi, J. Soulard, A. Cavagnino, and A. Boglietti, "Magnetic Materials Used in Electrical Machines: A Comparison and Selection Guide for Early Machine Design," *IEEE Ind. Appl. Mag.*, vol. 23, no. 6, pp. 21 – 28, Nov./Dec. 2017.

[9] Y. G. Guo, J. G. Zhu, P. A. Watterson, and W. Wu, "Development of a PM Transverse Flux Motor With Soft Magnetic Composite Core," *IEEE Trans. Energy Convers.*, vol. 21, no. 2, pp. 426 – 434, June 2006.

[10] J. Asama, T. Oiwa, T. Shinshi, and A. Chiba, "Experimental Evaluation for Core Loss Reduction of a Consequent-Pole Bearingless Disk Motor Using Soft Magnetic Composites," *IEEE Trans. Energy Convers.*, vol. 33, no. 1, pp. 324 – 332, Mar. 2018.

[11] SKF Bearing Calculator. [Online]. Available: http://webtools3.skf.com/BearingCalc/.

[12] K. W. Klontz, "Permanent Magnet Motor with Tested Efficiency Beyond Ultra-Premium/ IE5 Levels," in *Proc. ACEEE Summer Study on Energy Efficiency in Industry*, 2017, pp. 1 – 12.